Scientific Research Publishing

Journal of Power and Energy Engineering, 2022, 10, 31-55
https://www.scirp.org/journal/jpee
ISSN Online: 2327-5901
ISSN Print: 2327-588X

Observer-Based Disturbance Accommodation Control Strategy for Useful Lifetime Control and Structural Load Mitigation of Wind Turbines

Rutendo Goboza[1*], Jackson Githu Njiri[2], James Kuria Kimotho[3]

[1]Department of Mechatronic Engineering, Pan African University Institute for Basic Sciences, Technology and Innovation, Nairobi, Kenya
[2]Department of Mechatronic Engineering, Jomo Kenyatta University of Agriculture and Technology, Nairobi, Kenya
[3]Department of Mechanical Engineering, Jomo Kenyatta University of Agriculture and Technology, Nairobi, Kenya
Email: *rgoboz@gmail.com

How to cite this paper: Goboza, R., Njiri, J.G. and Kimotho, J.K. (2022) Observer-Based Disturbance Accommodation Control Strategy for Useful Lifetime Control and Structural Load Mitigation of Wind Turbines. *Journal of Power and Energy Engineering*, **10**, 31-55.
https://doi.org/10.4236/jpee.2022.107003

Received: May12, 2022
Accepted: July 25, 2022
Published: July 28, 2022

Abstract

Wind turbines undergo degradation due to various factors which induce stress, thereby leading to fatigue damage to various wind turbine components. In addition, the current increase in demand for electrical power has led to the development of large wind turbines, which result in increased structural loads, therefore, increasing the possibility of early failure due to fatigue load. This paper proposes a proportional integral observer (PI-Observer) based disturbance accommodation controller (DAC) with individual pitch control (IPC) for load mitigation to reduce components' damage and ensure the wind turbine is operational for the expected lifetime. The results indicate a reduction in blades' bending moments with a standard deviation of 15.9%, which positively impacts several other wind turbine subsystems. Therefore, the lifetime control strategy demonstrates effective structural load mitigation without compromise on power generation, thus, achieving a nominal lifetime control to inhibit premature failure.

Keywords

Disturbance Accommodation Control, Individual Pitch Control, Lifetime Control, Structural Load Mitigation

1. Introduction

Wind turbines are presently designed to be efficient and reliable for 20 years with possible extensions beyond that [1], but in most cases, there is a likelihood of failure before reaching this time due to fatigue damage. There are various

factors that cause extensive degradation of one or more components in the wind turbine, such as exposure to harsh environmental conditions and time varying gravitational, aerodynamics and inertia loads. Rotor blades, for example, can be obstructed by lightning strikes, vibrations, corrosion, and unsteady inflow wind speed [2]. These unsteady winds cause load fluctuations and cyclic loading which induce high torque, thus increasing stress on the blades. Cracks and corrosion on blades also reduce the efficiency of wind turbines. Although they can be modeled in design stages, predicting how a turbine will be impacted by the natural environment is difficult to achieve.

The tower, drivetrain, and foundation of the turbine are critical components in wind turbine, but rotor blades tend to bear more fatigue load. Therefore, fatigue if not monitored and controlled will result in downtime leading to losses both in electric power generation and in the cost of replacement or repairs.

Researchers have developed various models that monitor wind turbine and forecast the lifetime before it fails. The damage evaluation models are either model-based or data-driven [3]. These models forecast the occurrence of faults and enable planning for future maintenance schedules. The conventional analysis techniques for wind turbine blade fatigue include, but are not limited to, the Palmgren-Miner linear damage rule (Miner's rule) and the linear crack propagation. These conventional off-line cycle-based models require the load profile time history, hence, requiring large memory storage. However, the online models recently developed are more efficient and process data (extremum points) in real-time as they occur, thus requiring less memory storage [4].

Recently, several approaches have been employed to mitigate structural loads, with the main objective being performance and stability with less consideration of the effects of components' degradation. These effects need to be considered and compensated for during power production in order to realize better performance and control the operational lifetime of wind turbines. Though several control schemes for load mitigation have been proposed [5] [6], the major concern on how damage evaluation models can be used to control the wind turbine operational life without compromising power generation and regulation of speed has not been extensively discussed. Therefore, to control the lifetime of wind turbines, a trade-off between structural load mitigation and power generation and should be realized. The objective of the control scheme proposed in this paper is to control the remaining useful life of the wind turbine based on the damage accumulation on blades while realizing a trade-off between load mitigation and power/speed regulation.

Classical control schemes used collective pitch control to regulate the power/speed of wind turbines without considering varying aerodynamic load [7]. Individual pitch control (IPC) is a better option to improve system performance because it enables the control of both the asymmetric and symmetric aerodynamic loads. Asymmetric loads on blades induce excitation by a rotational frequency (1p) harmonic load [8] [9] as well as other loads acting on them hence

causing larger fatigue damage. However, with IPC the braking system of each blade can be individually considered (individual pitch angle control) to eliminate the need for a higher rating shaft brake and consequently improve system response by reducing the probability of failure even when one of the blades fails [5].

This paper proposes a Proportional Integral Observer (PI-Observer) based disturbance accommodation controller (DAC) with IPC for lifetime control of wind turbines. Due to wind speed variation, estimation of unknown disturbances and system state is realized by the observer while the DAC compensates for disturbances as well as regulation of speed in order to improve performance. For controller design, a 1.5 MW National Renewable Energy Laboratory (NREL) Fatigue, Aerodynamics, Structures, and Turbulence (FAST) reference wind turbine is used in this paper.

The structure of this paper is as follows; Section 2 gives a description of the NREL FAST reference wind turbine model used for designing the control strategy proposed. Section 3 gives a description of the damage evaluation algorithm adopted in this paper; then Section 4 describes the design of the (DAC) control scheme with IPC for structural load mitigation. Finally, Section 5 discusses the simulation results.

2. The Nrel Fast Wind Turbine Model Description

In this paper, one of the reference wind turbine models developed by NREL [10] is used for purposes of simulation to test and analyze the performance of the proposed observer-based control design. The 1.5 MW WindPACT model used in this paper is an upwind 3-bladed wind turbine with a horizontal axis and subjected to variable speed. The full specifications of the model are summarized in Table 1. The model has 24 degrees of freedom (DoFs) which defines its flexibility.

Table 1. Wind turbine specifications.

Rated rotor speed	20 rpm
Hub height	84.288 m
Configuration	3 blades, upwind
Cut_in, Rated, Cut_out wind speed	4 m/s, 12 m/s, 25 m/s
Gearbox ratio	87.965
Blade diameter	70 m
Rated power	1.5 MW
Blade pitch range	0 - 90˚
Pitch rate	10˚/s
Optimum tip-speed ratio (λ_{opt})	7.0
Maximum power coefficient (Cp_{max})	0.5
Optimal pitch angle (β_{opt})	2.6˚

The wind turbine motion nonlinear model in [10] is given by

$$M\left(\underline{q},\underline{u},t\right)\ddot{\underline{q}}+f\left(\underline{q},\dot{\underline{q}},\underline{u},\underline{u}_d,t\right)=0, \tag{1}$$

where, M represents the mass matrix containing components of mass and inertia, $\underline{u}$ is the control input, t is time, f denotes the nonlinear function of the DoFs enabled, q and $\dot{q}$ are the first and second derivatives of the enabled DoFs and $\underline{u}_d$ is the disturbance input. The nonlinear model is linearized in FAST which is a two-step process of computing the realized steady state of the specified operating points (the individual pitch 20˚, wind speed 18 m/s, rotor speed 20 rpm) of the enabled DoFs followed by the numerical linearization with regards to the computed steady states in order to obtain the linear model matrices. For controller design in this paper, only 5 DoFs are enabled which are relevant for rotor blades and tower structural load mitigation. The enabled DoFs are the first tower fore-aft mode (τ_f), variable speed generator (ψ) and the first flapwise bending mode of blade 1 (ς_1), blade 2 (ς_2) and blade 3 (ς_3). The linearized state space model of the wind turbine is denoted by

$$\dot{x}_m = A_m x_m + B_m u_m + B_{m_d} u_{m_d}, \tag{2a}$$

$$y_m = C_m x_m, \tag{2b}$$

where, A_m is the state matrix, B_m is the control input matrix, B_{m_d} represents the unknown disturbance matrix, C_m is the output matrix, x_m is the state vector, u_m is the perturbed input vector of individual pitch angles, u_{m_d} is the unknown disturbance vector, and y_m is the measured output vector. The subscript m denotes that the linear model is expressed in both rotating and fixed reference coordinates.

The linear model yielded is highly periodic about the azimuth position due to various factors such as vertical wind shear and tower shadow [11]. The periodicity effects even tend to be more pronounced as the wind turbine ratings go up (bigger sized wind turbines) and therefore Multi blade coordinate (MBC) transformation is carried out to account for the wind turbine periodic dynamics during controller design. The multi-blade coordinate transformation integrates the dynamics of individual blades (rotating coordinate frame) and expresses it in a fixed nonrotating frame [11]. After transformation, the reduced order model is averaged in order to realize a weakly periodic linear time-invariant (LTI) model denoted by

$$\dot{x}_n = A_n x_n + B_n u_n + B_{n_d} u_{n_d}, \tag{3a}$$

$$y_n = C_n x_n, \tag{3b}$$

where, subscript n indicates the nominal LTI model.

To obtain pitch actuation for (IPC), there is a need for an actuator model since it is not embedded within the NREL FAST model. The actuator model as in [12] is given by

$$\frac{\beta}{\beta_g} = \frac{1}{s\tau_\beta + 1}, \tag{4}$$

where, β is the actual pitch angle that controls the rotor blade, β_g is the generated pitch angle, and τ_β denotes the time constant. The blade pitch actuator model for each blade in individual pitch control is given by

$$\begin{bmatrix} \dot{\beta}_1 \\ \dot{\beta}_2 \\ \dot{\beta}_3 \end{bmatrix} = \begin{bmatrix} -\frac{1}{\tau\beta_1} & 0 & 0 \\ 0 & -\frac{1}{\tau\beta_2} & 0 \\ 0 & 0 & -\frac{1}{\tau\beta_3} \end{bmatrix} \begin{bmatrix} \beta_1 \\ \beta_2 \\ \beta_3 \end{bmatrix} + \begin{bmatrix} \frac{1}{\tau\beta_1} & 0 & 0 \\ 0 & \frac{1}{\tau\beta_2} & 0 \\ 0 & 0 & \frac{1}{\tau\beta_3} \end{bmatrix} \begin{bmatrix} \beta_{g_1} \\ \beta_{g_2} \\ \beta_{g_3} \end{bmatrix}. \tag{5}$$

The above equation can be simplified to a generalized state space form as

$$\dot{x}_a = A_a x_a + B_a u_a, \tag{6a}$$

$$y_a = C_a x_a, \tag{6b}$$

where, $x_a = \begin{bmatrix} \Delta\beta_1 & \Delta\beta_2 & \Delta\beta_3 \end{bmatrix}^{\mathrm{T}}$, $u_a = \begin{bmatrix} \Delta\beta_{g_1} & \Delta\beta_{g_2} & \Delta\beta_{g_3} \end{bmatrix}^{\mathrm{T}}$ and $y_a = x_a$.

According to [13], the wind turbine LTI model is augmented with the pitch actuator to account for pitching actuation. Therefore, the LTI augmented model with pitch actuator is given by

$$\begin{bmatrix} \dot{x}_n \\ \dot{x}_a \end{bmatrix} = \begin{bmatrix} A_n & B_n C_a \\ 0 & A_a \end{bmatrix} \begin{bmatrix} x_n \\ x_a \end{bmatrix} + \begin{bmatrix} 0 \\ B_a \end{bmatrix} u_a + \begin{bmatrix} B_{n_d} \\ 0 \end{bmatrix} u_{n_d}, \tag{7a}$$

$$\begin{bmatrix} y_n \\ y_a \end{bmatrix} = \begin{bmatrix} C_n & 0 \\ 0 & C_a \end{bmatrix} \begin{bmatrix} x_n \\ x_a \end{bmatrix}. \tag{7b}$$

The above augmented model with pitch actuator is used for the design of the proposed (DAC) with an individual pitch controller for lifetime control and can be simplified to the form

$$\dot{x} = Ax + Bu + B_d u_d, \tag{8a}$$

$$y = Cx. \tag{8b}$$

3. Online Damage Evaluation

Variable wind speeds cause load fluctuations in wind turbine components which results in fatigue damage. Therefore, it is important to monitor the degradation of the wind turbine components [3] in order to analyze and control the degradation to prevent components' failure before the expected lifetime. Cycle counting methods are greatly used for fatigue damage analysis [4], especially in unpredictable load fluctuation applications such as wind turbine operation. These methods are able to simplify the varying load data and can be easily combined with Miner's rule for analysis purposes. The general machine components' damage degradation is expressed by the Wöhler equation, as indicated in [14] is given by

$$s^m N = K, \tag{9}$$

where, s is the stress range amplitude, m is the Wöhler coefficient which is 3 for steel components and 10 for fiber composite material components such as rotor blades, N the number of cycles to failure for a given stress range s and K as a con-

stant parameter that is material specific [14].

Several cycle counting methods have been developed, which include peak counting, simple range counting, level crossing counting, and rainflow counting [15]. This paper adopts the improved online rainflow counting method for the efficient processing of unpredictable load fluctuations and less memory storage requirement. The rainflow counting algorithm generates load cycles (half or full cycles) that are equivalent to the local minima and maxima values of the arbitrary loads. Therefore, the damage degradation D_k when the Rainflow counting algorithm and the Miner's rule are combined gives

$$D_k = \sum_{i=1}^{k} d_i = \sum_{i=1}^{k} \frac{n_i}{N_i} = \sum_{i=1}^{k} \frac{n_i s_i^m}{K}, \tag{10}$$

where, k is the entire number of cycles, d_i the damage equivalent to a specified stress cycle, n_i the number of load cycles applied, N_i the number of cycles the material endures until failure and s_i the stress range corresponding to the i_{th} stress cycle. Components are said to have no damage at $D_k = 0$ and when they reach $D_k = 1$ they are considered to have reached the end of their lifetime. For wind turbine components, the designed service lifetime is at least 20 years, with the components reaching the end of life after roughly being subjected to between 10^8 and 10^9 load cycles [16].

If the wind turbine component's operational lifetime according to the manufacturer is given, then the Remaining Useful Lifetime (RUL) of the component as in [17] can be calculated as

$$\text{RUL} = L_e - T_k = T_k \left(\frac{D_d}{D_k} - 1 \right), \tag{11}$$

where, L_e is the estimated lifetime of the wind turbine components, T_k is the current time step, D_d is the damage accumulated value at the design lifetime, and D_k denotes the accumulated damage at every time step. The estimated lifetime L_e is given by

$$L_e = \frac{T_k}{D_k} D_d . \tag{12}$$

This conventional method requires the entire time series load history in order to determine the equivalent load cycles, which requires large memory storage. Therefore, the improved real-time rainflow counting algorithm (RFC) by [4] becomes a more efficient method. The online RFC algorithm adopted in this paper is for damage evaluation of blade root moments in real-time as they occur. The algorithm processes data with the help of two flexible stacks or buffers for storage and processing and employs a 3-point counting rule for detecting the maxima and minima data values as it applies a recursive mode algorithm as stated in [4]. Once the system begins operation and the load profile is detected, the 3-point counting rule identifies each extremal value as it comes, differentiates the maximum value from the minimum value then directs each value to its respective buffer and generates the equivalent cycle (half or full cycle) as depicted by **Figure 1**.

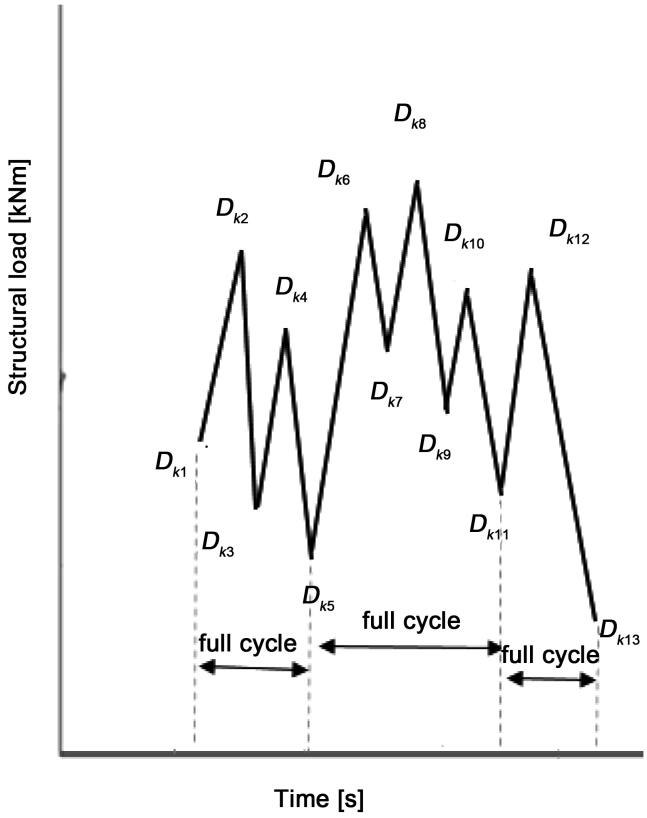

Figure 1. Online rainflow counting algorithm implementation [4].

The first extremum load values minima (D_{k_1}) and maxima (D_{k_2}) are defined and compared by the 3-point counting rule for purposes of identifying which storage buffer each value is to be stored in as explained in [4]. When the next value (D_{k_3}) a minima value arrives, the 3-point rule defines its stack and compares it to the other value already stored within the same buffer. Since there is only one maxima entry a half cycle is then decided which is ($D_{k_2} - D_{k_1}$) and the old minima value is eliminated. The process continues as (D_{k_4}) arrives making two entries in the maxima stack then (D_{k_5}) arrives which then a full cycle is decided ($D_{k_4} - D_{k_3}$) as two maxima values are in the maxima stack. The algorithm code carries on working on the data as it arrives comparing values in stacks and defining half and full cycles as shown in **Figure 1**.

4. Observer-Based Disturbance Accommodation Control Strategy

The proposed PI-Observer based disturbance accommodation control scheme with individual pitch control with an integrated online damage evaluation model is described here. A two control loop design is adopted as shown in **Figure 2**.

The first loop is designed for the regulation of generator speed by means of generating nominal demanded pitch angle which reduces the aerodynamic power coefficient in the high-speed region, thus, maintaining the rotor rotational speed about its rated value as the design in [18]. The second loop is utilized for

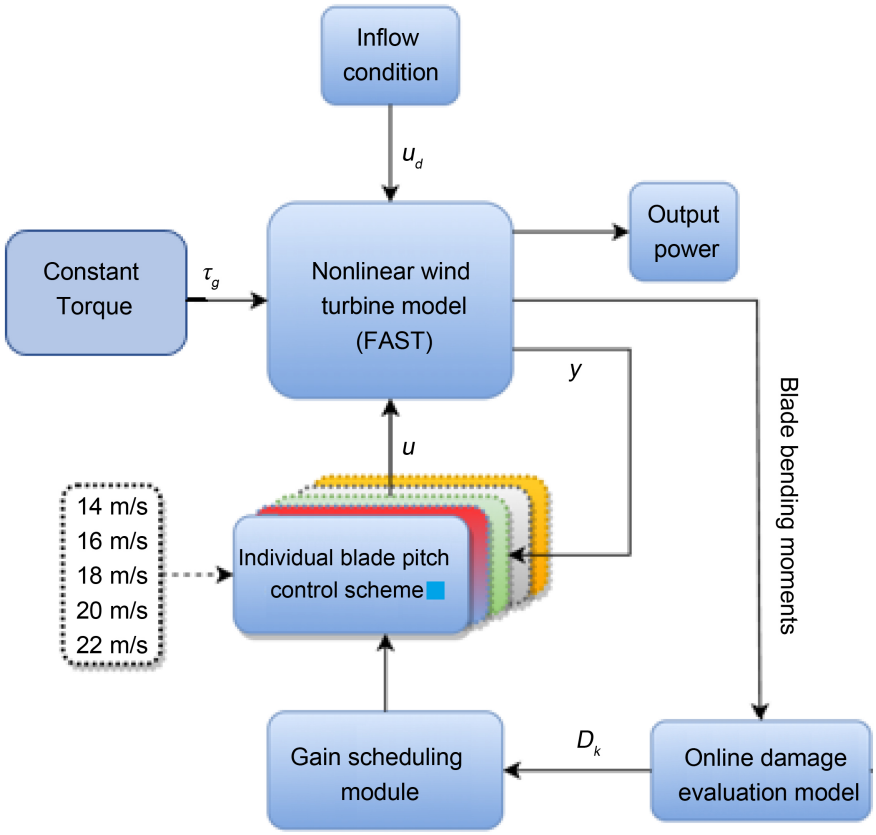

Figure 2. DAC with IPC control strategy.

structural load mitigation in blades by minimizing blade bending moments as a result of perturbing individual pitch angles around the nominal control signal. Here, several IPCs are designed for structural load reduction. The LTI model used for control design obtained after linearization, realizes a controller that is more efficient within the defined operating points of rotor speed 20 rpm, wind speed 18 m/s and pitch angle 20˚; hence, the need to design controllers linearized about a range of operating points spreading between the above rated wind speed region and the cut-out wind speed region. In this paper, the following wind speeds above the rated speed region were selected: 14 m/s, 16 m/s, 18 m/s, 20 m/s, and 22 m/s. Because of varying wind speed and inherent measurement noise, the PI-Observer estimates unknown disturbances and reconstructs the system state. The disturbance accommodation control compensates for the disturbance, fluctuating incoming wind, and regulates the power/speed of the wind turbine [19].

To control the RUL of a wind turbine, the online damage evaluation model determines damage accumulation during wind turbine operation. Gain scheduling module switches between IPCs depending on the predefined damage accumulation thresholds of bending moments. Here, the higher damage accumulation threshold will activate the controller with higher load mitigation capability. The gain scheduling module is able to monitor the damage accumulation so as to determine the changes in the operational ranges by varying the gain of the individual pitch controller [19]. This enables the proposed control scheme to be

able to achieve a trade-off between structural load mitigation and power/speed regulation, thereby inhibiting premature failure before the expected lifetime.

4.1. Proportional Integral Observer

In this paper, a PI-Observer is used for wind speed estimation and system state reconstruction. The Proportional Integral Observer comprises the integral feedback loop for error estimation as well as for the realization of the system state, and the proportional feedback loop as in **Figure 3**. With the basis of the deterministic nature of the plant, the PI-Observer is capable of reconstructing unknown/unmeasurable varying wind speed by using outputs measurements [20]. The observer attains wind speed estimation in a two-step process, which begins with the estimation of a fictitious disturbance component which is computed as a perturbed hub-height wind speed. Then follows adding the computed wind speed component to the nominal speed to realize its instantaneous value [21].

The dynamic model of unknown disturbance is expressed as

$$\dot{z}_d = F_{z_d}, \tag{13a}$$

$$u_d = H_{z_d}, \tag{13b}$$

where, z_d denotes the disturbance states, u_d is the unknown disturbance

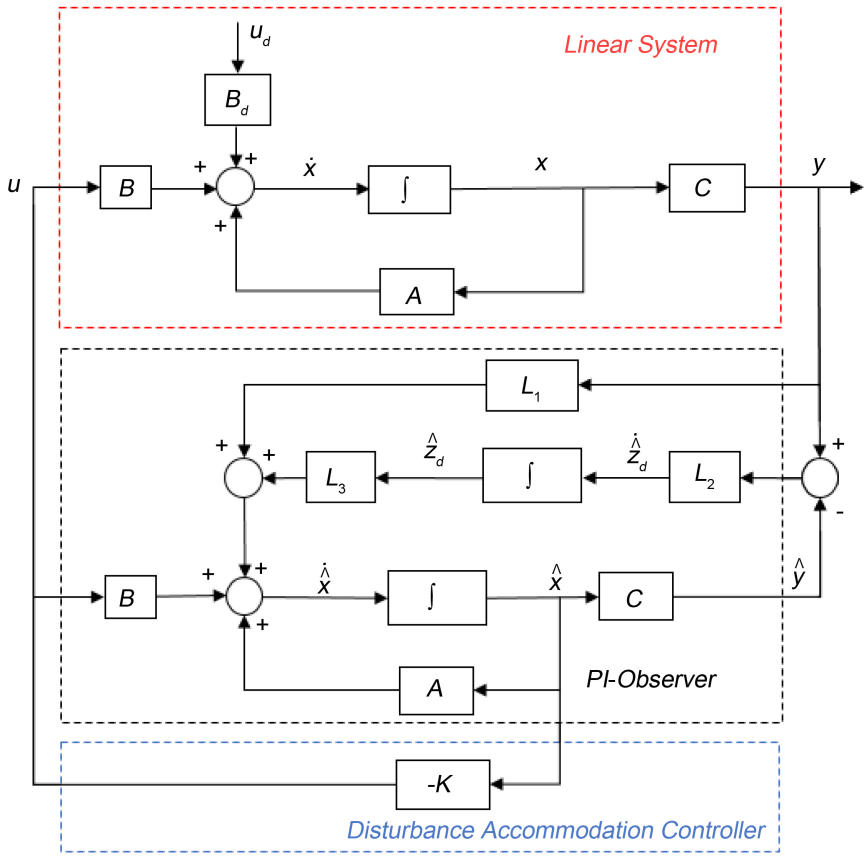

Figure 3. Example PI-obserever structure with controller.

vector, and F and H are the matrices of appropriate dimensions. Therefore, the disturbance dynamic model as indicated in [21] is given by

$$\begin{bmatrix} \dot{x} \\ \dot{z}_d \end{bmatrix} = \begin{bmatrix} A & B_d H \\ 0 & F \end{bmatrix} \begin{bmatrix} x \\ z_d \end{bmatrix} + \begin{bmatrix} B \\ 0 \end{bmatrix} u, \tag{14a}$$

$$y = \begin{bmatrix} C & 0 \end{bmatrix} \begin{bmatrix} x \\ z_d \end{bmatrix}, \tag{14b}$$

where, A is the state matrix, B is the control input matrix, B_d represents the unknown disturbance matrix, C is the output matrix, x is the state vector, u is the input vector of individual pitch angles, and y is the measured output vector.

Therefore, the PI-Observer dynamics equation is given by

$$\dot{\hat{x}} = A\hat{x} + B_d H_{\hat{z}_d} + B_u + L_1 \left(y - \hat{y} \right), \tag{15a}$$

$$\dot{\hat{z}}_d = F_{\hat{z}_d} + L_2 \left(y - \hat{y} \right), \tag{15b}$$

where, L_1 is the proportional loop gain matrix, L_2 is the integral loop gain matrix and $\hat{y} = C\hat{x}$.

The observer dynamics can be described in matrix form as

$$\begin{bmatrix} \dot{\hat{x}} \\ \dot{\hat{z}}_d \end{bmatrix} = \begin{bmatrix} A & B_d H \\ 0 & F \end{bmatrix} \begin{bmatrix} \hat{x} \\ \hat{z}_d \end{bmatrix} + \begin{bmatrix} B \\ 0 \end{bmatrix} u + \begin{bmatrix} L_1 \\ L_2 \end{bmatrix} \left(y - \hat{y} \right), \tag{16a}$$

$$\hat{y} = \begin{bmatrix} C & 0 \end{bmatrix} \begin{bmatrix} \hat{x} \\ \hat{z}_d \end{bmatrix}. \tag{16b}$$

4.2. Disturbance Accommodation Controller

To obtain the pitch control and be able to realize mitigation of structural loads, a full state multi-variable feedback controller is required. The full state feedback controller is given by

$$u = -\begin{bmatrix} K_x & K_d \end{bmatrix} \begin{bmatrix} x \\ z_d \end{bmatrix}, \tag{17}$$

where, x denotes the system states, z_d is the unknown disturbances, $-K_x$ is the system controller gain and $-K_d$ is the disturbance controller gain. Therefore $-K_x x$ is for regulation control of the system in order to improve performance, while $-K_d z_d$ is for disturbance compensation, fluctuating incoming wind [22]. However, because of some inaccessible and unmeasurable variables as well as unknown disturbances that are ultimately estimated by the observer, the full state feedback controller with estimated states is given by

$$u = -\begin{bmatrix} K_x & K_d \end{bmatrix} \begin{bmatrix} \hat{x} \\ \hat{z}_d \end{bmatrix}. \tag{18}$$

The two main methods for disturbance accommodation developed are static and dynamic approaches. A good disturbance compensation approach ensures good system response and disturbance effects minimization. For the static disturbance approach as stated in [22], compensation of disturbance effects can

only be possible under the condition that

$$BK_d + B_d H = 0. \tag{19}$$

Therefore, this makes it realistically impossible to reject the disturbance effects with this approach unless disturbance signals and input control signals enter the system by the same channel [23] [24].

The dynamic disturbance approach that is adopted in this paper, compliments the static disturbance in its limitations and makes use of all system states for disturbance compensation [23]. The dynamic disturbance model is given by

$$\dot{z}_d = Fz_d + \delta_\epsilon x, \tag{20}$$

where F is the corresponding distribution matrix of unknown disturbances and δ_ϵ is the coupler of unknown disturbances and system states.

Therefore, the plant model with dynamic disturbance compensation is expressed by

$$\begin{bmatrix} \dot{x} \\ \dot{z}_d \end{bmatrix} = \begin{bmatrix} A & B_d H \\ \delta_\epsilon & F \end{bmatrix} \begin{bmatrix} x \\ z_d \end{bmatrix} + \begin{bmatrix} B \\ 0 \end{bmatrix} u, \tag{21}$$

where, A, B and F, δ_ϵ are assumed to be controllable.

5. Results and Discussion

Two different wind profiles that are generated by the NREL TurbSim simulation code are adopted in this paper to excite the wind turbine dynamics for 100 seconds. The stochastic wind profile used, shown in **Figure 4(a)**, has vertical wind shear, a mean speed of 18 m/s, and a power exponent of 0.143. Wind shear is often assigned a power exponent of 0.143 for a well-mixed atmosphere, over open and flat terrain while higher power law exponent values are usually assigned for vegetated surfaces with light wind speeds [25]. The step wind profile used varies in steps from 14 m/s to 22 m/s as shown in **Figure 4(b)**. A comparison of the actual hub height wind speed plot and that of the wind speed estimated by the PI-Observer is shown in **Figure 5**. While the general flow of the estimated wind speed follows the actual, some large deviations are observed of a standard deviation of 22.8% as the wind speed diverges from the nominal operating point value that the system was linearized at.

The performance of each of the individual blade pitch controllers (IPC) with varying load capabilities integrated with the damage evaluation model is compared with the performance of the lifetime control (DAC with IPC) model integrated with the damage evaluation model and gain scheduling module is shown in **Figure 6**.

Controller 1 (C1) describes a case where speed/power regulation and structural load mitigation is achieved, but with a penalty of a steep damage accumulation at certain intervals. Controller 2 (C2) and Controller 4 (C4) have good speed power regulation ability though with low load mitigation ability. Controller 3 (C3) has strong structural load mitigation ability, however, with a compromise on power/speed regulation. Controller 5 (C5) represents fairly good structural

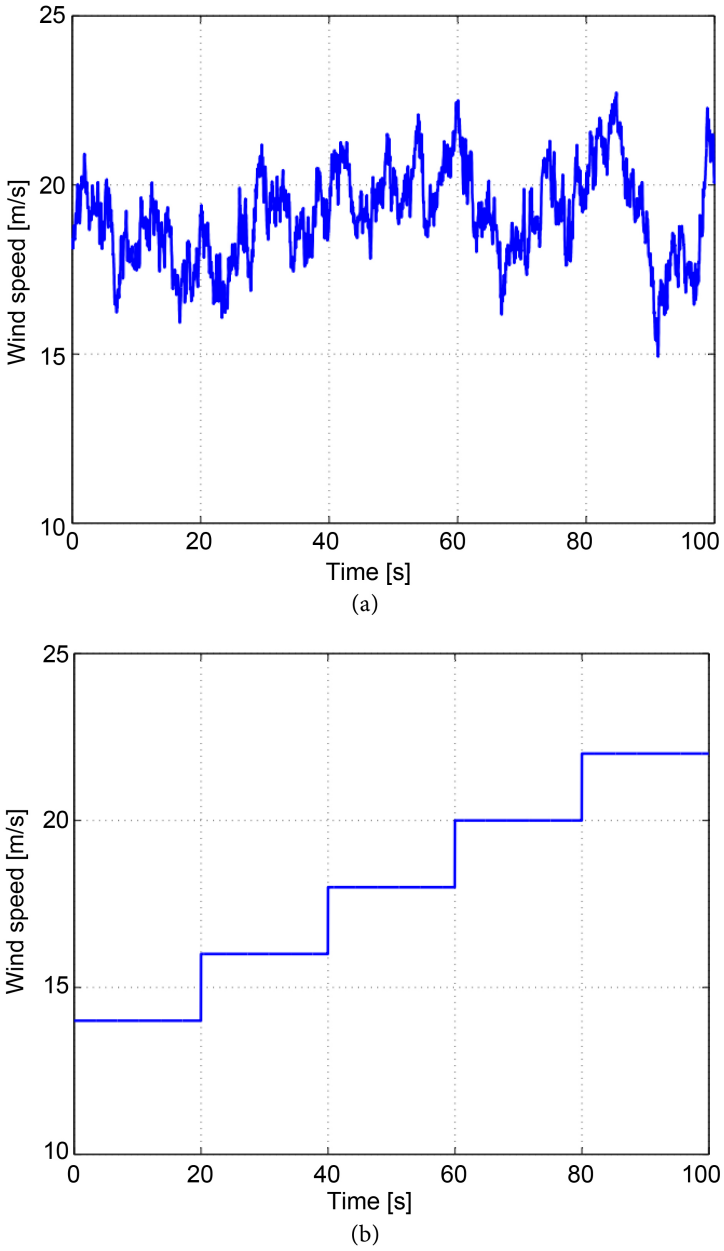

Figure 4. Hub height wind speed. (a) Stochastic wind profile. (b) Step wind profile.

load mitigation and speed/power regulation. The damage limit considered is the D_k value at the end of life: simulation time 100 seconds, for a case where an optimum trade-off between load mitigation and speed regulation was achieved. This was realized in the C1 case. Without the lifetime control scheme, the wind turbine controlled by C2 loses its functionality at about 74 seconds, C3 at about 34 seconds, C4 at about 63 seconds and C5 at about 88 seconds. The lifetime control strategy controls the blades' damage accumulation and delays degradation thus, enabling the blades to reach the damage limit at the expected lifetime of 100 seconds. Though C1 attains almost the same results as the lifetime control

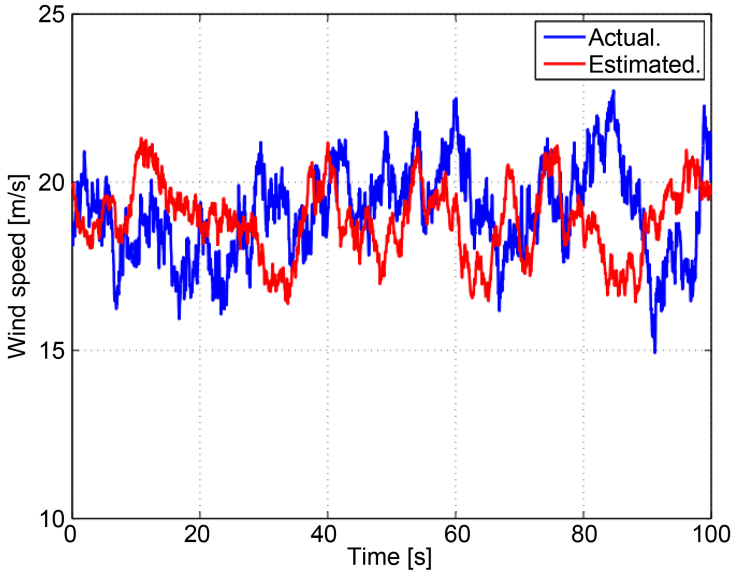

Figure 5. Wind speed estimation.

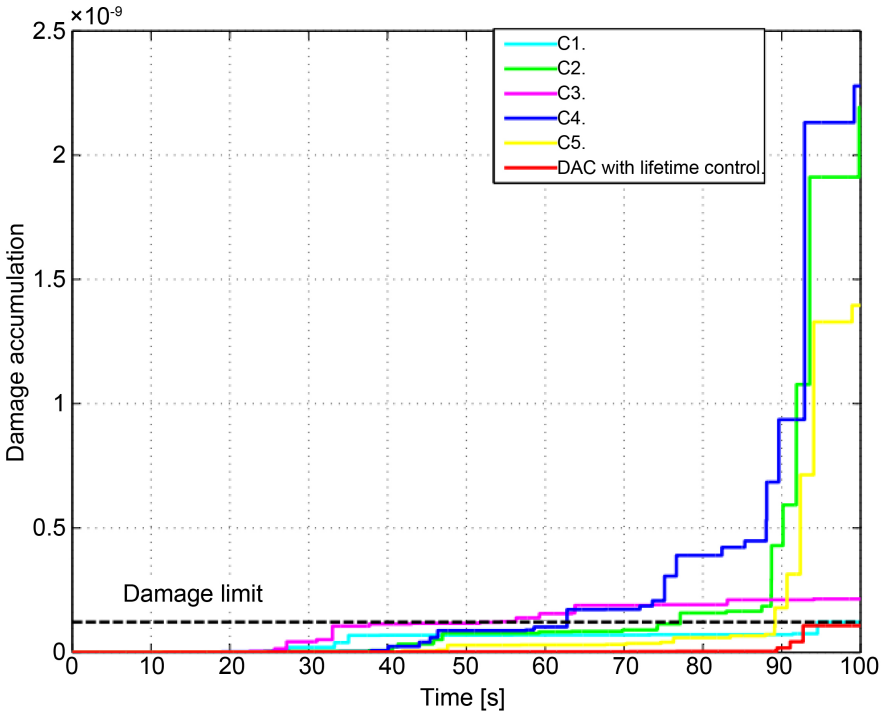

Figure 6. Control performance comparison.

scheme, the damage accumulation when the lifetime control model is in operation is gradual and spread over the lifetime due to the dynamic switching of different individual pitch controllers depending on load damage in blades that occurs during operation. Observations in [17] [18], [19] demonstrates the capabilities of different controller designs in mitigating structural loads.

A significant reduction of bending moments when lifetime control scheme is adopted can be observed in **Figure 7**. The blade flapwise moments profile in

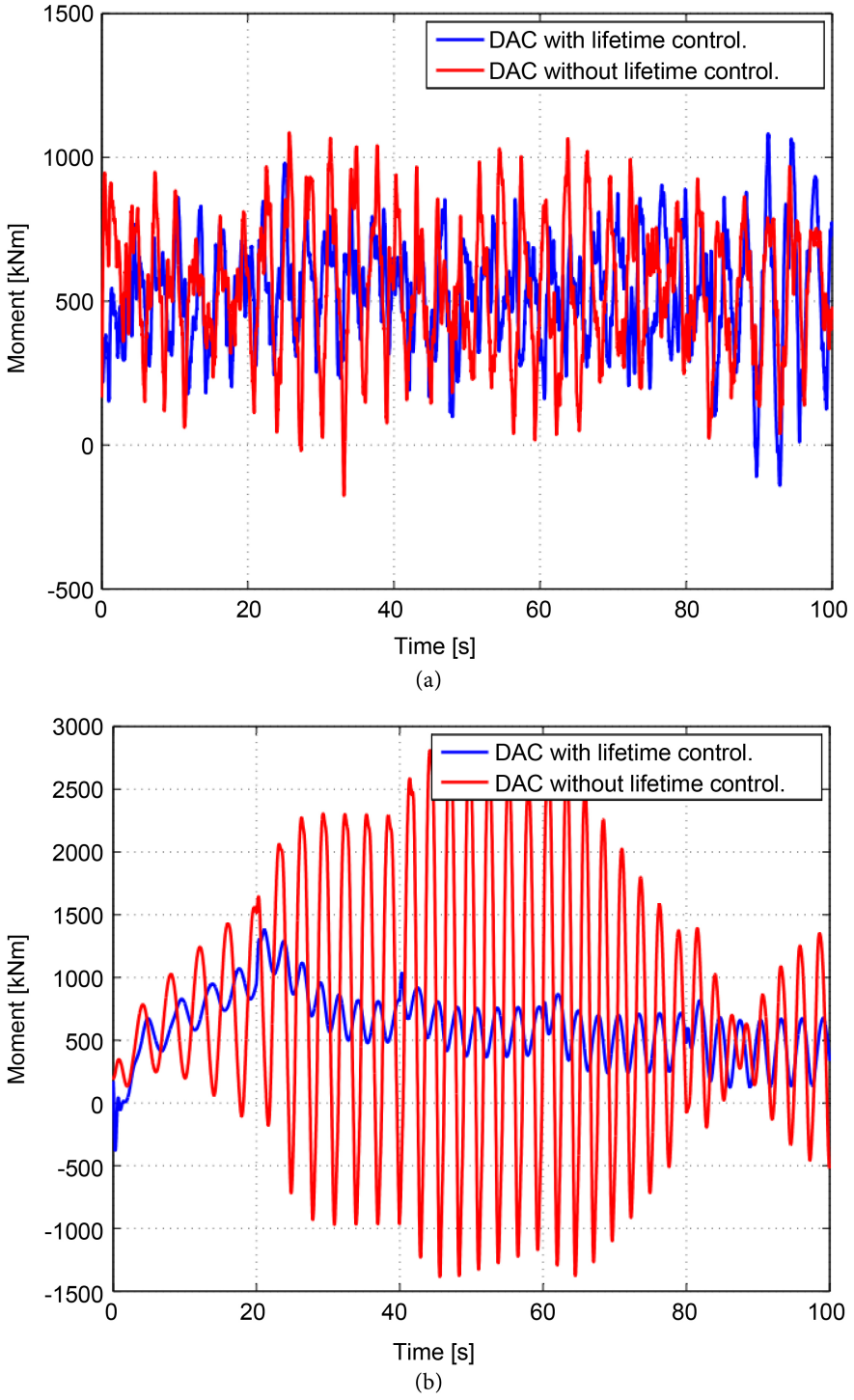

Figure 7. Blade flapwise moments. (a) Blade 1 flapwise bending moments (stochastic wind); (b) Blade 1 flapwise bending moments (step wind).

Figure 7(a) is influenced by the wind profile used for excitation as the results profile tries to track the stochastic wind profile.

The flapwise bending moments generally decrease throughout the simulation when the life time control is employed, with a standard deviation of 15.9%. An

increase in structural load as wind speed increases can be observed in **Figure 7(b)**. For step wind profile in **Figure 7(b)**, when DAC without lifetime control is employed, moments show a steep increase at every wind speed step increase from the beginning until about 60 seconds when wind speed increases to 20 m/s then the moments begin to decrease. When the lifetime control is employed, the flapwise moments increase up to about 20 seconds (a 16 m/s step wind speed increase) then moments decrease and become stable generally with slight fluctuations at every wind speed step increase. The lifetime control reduces the flapwise bending moments with a standard deviation of 72.6%. Similar observations are also supported by the results achieved in [17] [18] and [19] [26].

A reduction in the blade damage accumulation is observed when the lifetime control scheme is employed as illustrated in **Figure 8**. The accumulated damage was reduced by almost 50%. A significant reduction in blade damage accumulation demonstrates that control of bending moments in blades mitigates structural loads in blades and ultimately reduces damage accumulation. Therefore, showing that the lifetime control strategy delays degradation hence ensuring the blades do not fail before the expected lifetime. Various studies in [17] [18] and [19] [26] also support that reducing structural loads in blades reduces damage accumulation.

Most control strategies usually compromise on power production, but this study aims to achieve a tradeoff between load mitigation and power/speed regulation. While improvement in damage accumulation has been realized due to reduction in blade bending moments, there is a need to demonstrate that this improvement in damage accumulation does not compromise the power production

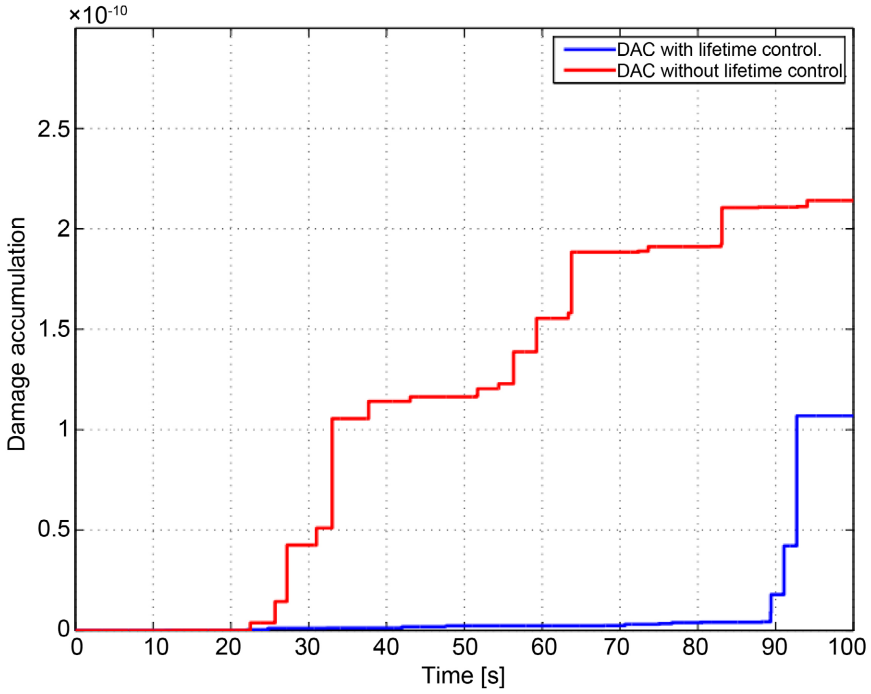

Figure 8. Blade damage accumulation.

of the wind turbine. Power regulation control is achieved for both stochastic wind profile excitation as shown in Figure 9(a) and step wind profile excitation as shown in Figure 9(b).

This is shown by the generator power being maintained about the rated value. Some small deviations are observed in the performance of each controller in both figures. In Figure 9(a), a difference of a standard deviation of 16.3% is observed while in Figure 9(b), a difference of a standard deviation of 3.4% is observed. The output power variation is generally related to the profile of the wind

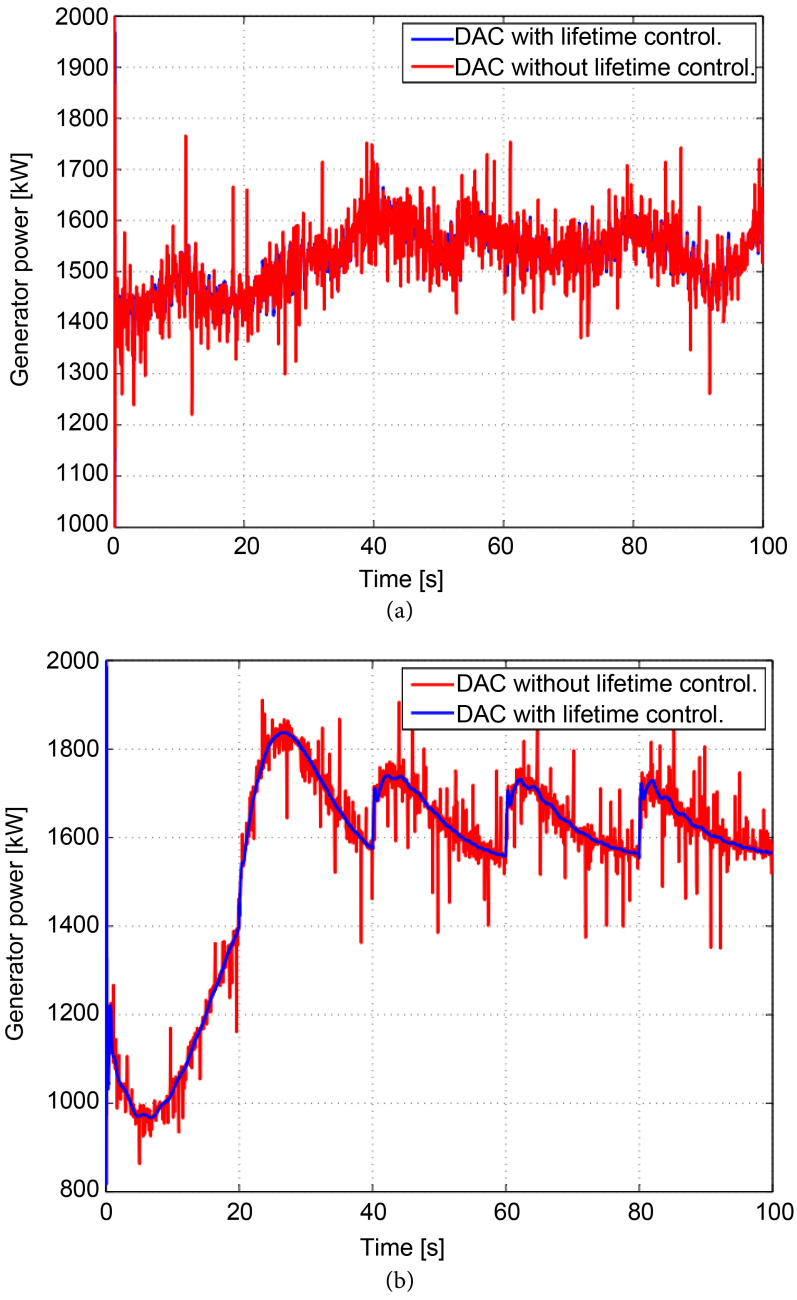

Figure 9. Generator performance. (a) Generator power (stochastic wind). (b) Generator power (step wind).

profile used for excitation. With a stochastic wind profile, the output power tries to follow the incoming wind profile but because of wind speed variations and inertia loads, perfect tracking is not possible. The power produced drops slightly as shown in **Figure 9(a)**, when lifetime control strategy is employed. But generally, the power regulation is stable about the rated power value throughout with fewer fluctuations. For step wind excitation shown in **Figure 9(b)**, a step in output power is observed at every step wind speed increase, as the value is regulated to the rated power value due to transient effects diminishing. Generator performance improvement is noted with the use of lifetime control strategy as the power output profile is more stable (fewer fluctuations) compared to DAC without lifetime strategy. Power regulation is realized due to the IPC improving the transient performance. This indicates that the control strategy in this paper is able to efficiently mitigate structural loads without compromising the generator power performance. Structural load mitigation and power regulation are also achieved in [17] and [19] but a slight compromise on power generation was noted in [19].

Tower loads can be mitigated by various methods, however tower load mitigation in this paper is limited to blade load mitigation. Therefore, it is necessary to evaluate the effects of blades' load mitigation on tower moments of the wind turbine. These effects of blade load mitigation on various wind turbine components are evident due to the existence of couplings amongst different modes and components of wind turbine. Because of very strong coupling between blades' flapwise mode and tower fore-aft bending mode, a reduction in tower fore-aft bending moments are evaluated in **Figure 10**.

The results show that tower fore-aft moments variation is also generally related to the profile of the wind profile used for excitation. For the stochastic wind profile in **Figure 10(a)**, a subtle difference in the tower fore-aft moments are observed mostly, though some huge deviations which quickly subside are detected at the beginning due to transient effects. With lifetime control, the tower fore-aft moments reduced with a standard deviation of 45.8%. For the step wind profile excitation in **Figure 10(b)**, a step increase in tower fore-aft moments are observed at every step wind speed increase for the two controllers in comparison. However, when lifetime control is employed, the controller is able to regulate the moments to be stable and settle at an almost similar level after every step increase. With DAC without lifetime control, the moments are reduced but fail to settle to similar level. The lifetime control strategy reduces the tower fore-aft moments with a standard deviation of 4.4% in **Figure 10(b)**. These results are supported by studies in [17] [19] which show that tower fore-aft moments are influenced by the blade load mitigation.

Tower side-to-side moments also demonstrate improvement when lifetime control strategy is employed, as shown in **Figure 11**. A difference in the side-to-side moments from controllers in comparison is visible for stochastic wind profile excitation. The tower side-to-side moments reduced with a standard deviation of 14.4% as illustrated in **Figure 11(a)** when the lifetime control is employed. For the step wind profile in **Figure 11(b)**, the step wind speed increase does

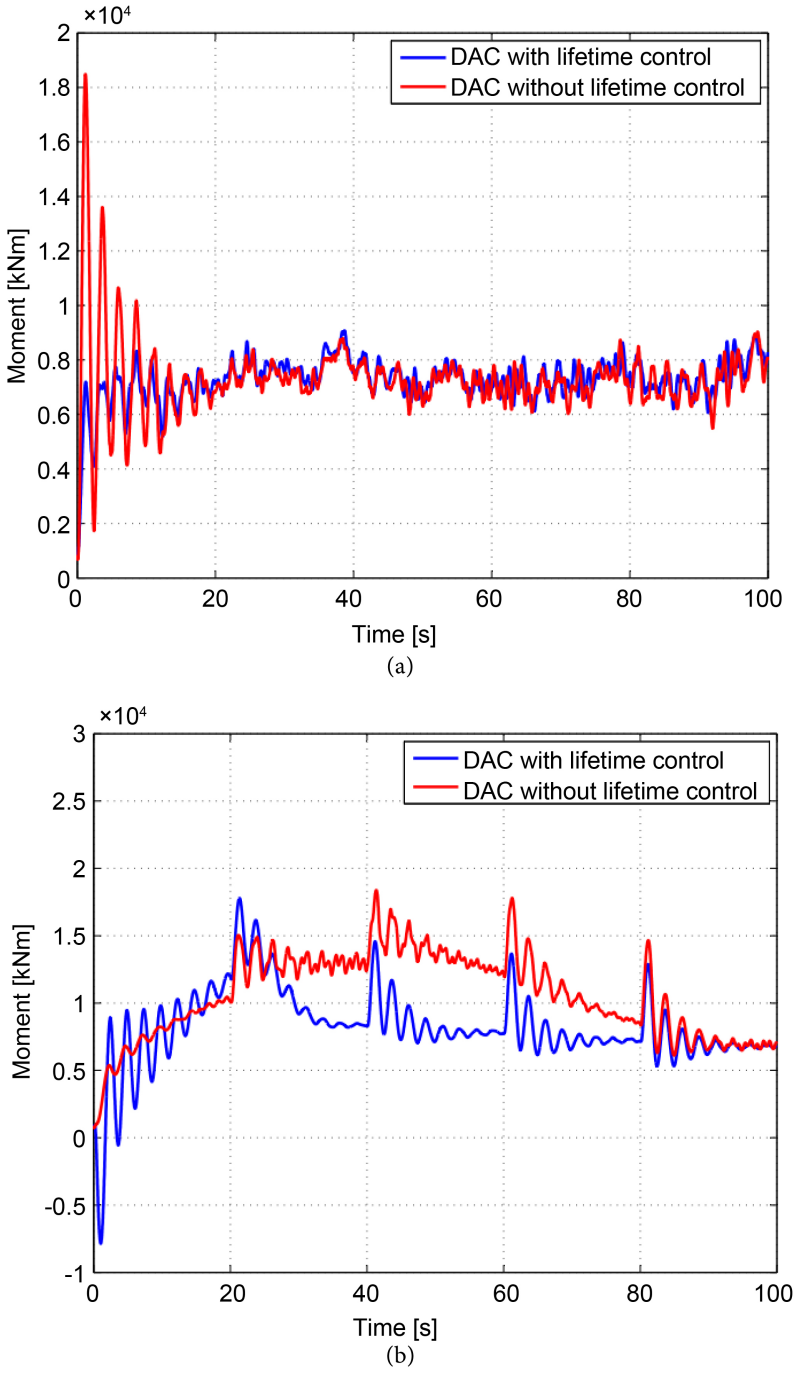

Figure 10. Tower fore-aft bending moments. (a) Tower fore-aft moments (stochastic wind). (b) Tower fore-aft moments (step wind).

not strongly influence the moments though the moments continuously reduce due to lifetime control use. A reduction in tower side-to-side moments with a standard deviation of 20.1% demonstrates the efficiency of the lifetime control in mitigating tower moments. Studies in [19] demonstrated similar findings, with tower side-to-side moments improving when a model under study was employed.

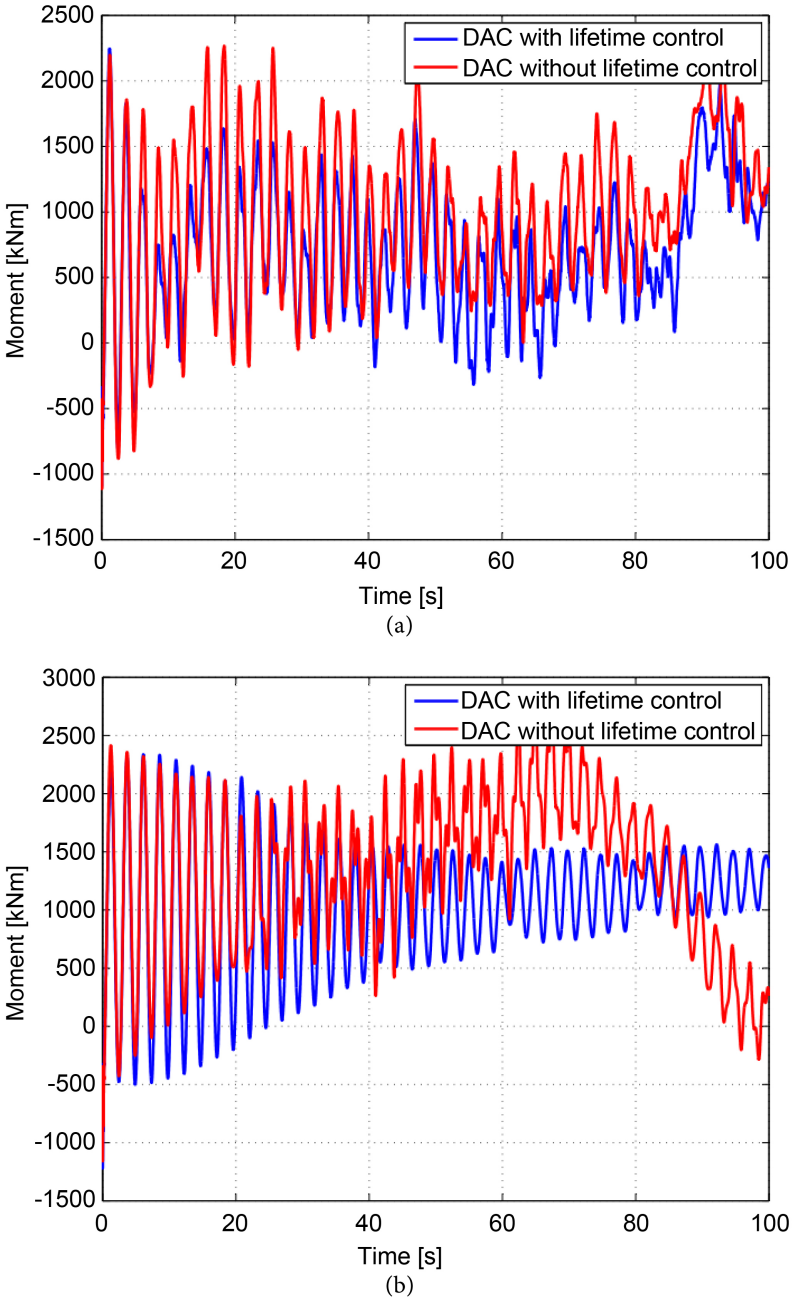

Figure 11. Tower side-to-side bending moments. (a) Tower side-to-side moments (stochastic wind). (b) Tower side-to-side moments (step wind).

Due to the coupling between blade flapwise deflection mode and the tower fore-aft deflection mode, evaluation of the effects of the control scheme on tower deflection is essential. Tower fore-aft deflection variations are strongly influenced by the profile of the wind profile used for excitation. In **Figure 12(a)**, a subtle difference in the tower fore-aft deflection between the two controllers is observed though with huge transient deflection at the start of simulation which subsides within about 10 seconds. An improvement in tower deflection is observed with tower fore-aft deflections reducing with a standard deviation of

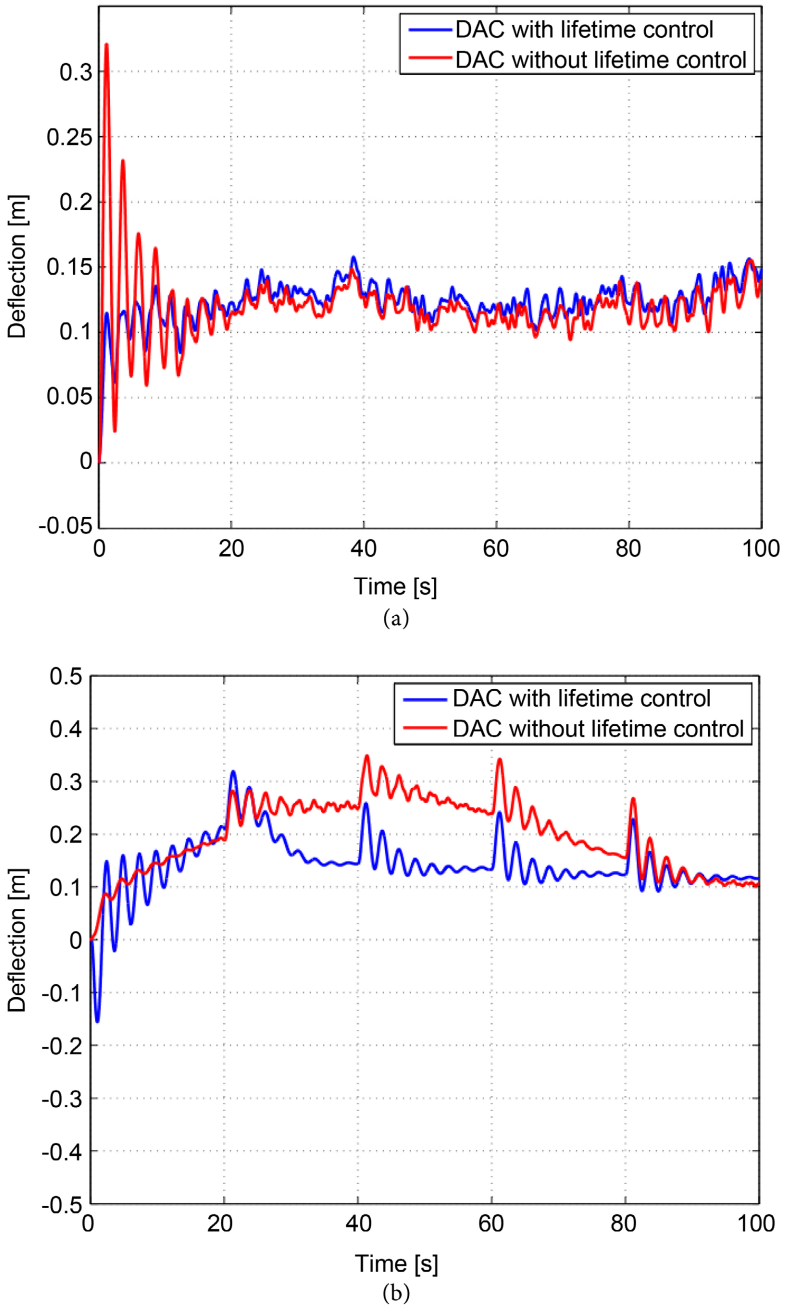

Figure 12. Tower fore-aft deflection. (a) Tower fore-aft deflection (stochastic wind. (b) Tower fore-aft deflection (step wind).

41.6% when the lifetime control scheme is employed. In Figure 12(b), an increase in tower fore-aft deflection value (transient deflection) is observed at every step wind speed change for both controllers. However, when lifetime control is employed, the controller is able to regulate and stabilize the deflections to an almost similar value after every step increase. With DAC without lifetime control, the deflections are reduced but fail to settle at a similar deflection level. The lifetime control strategy reduces the tower fore-aft deflections for step wind profile excitation with a standard deviation of 18.4% as in Figure 12(b).

Figure 13 exhibits the performance of the lifetime control and the DAC without lifetime control in regards to mitigating tower side-to-side deflection. The results indicate that the wind profile used for excitation has less influence on the tower side-to-side deflection profile.

In Figure 13(a), some significant variations in tower side-to-side deflection between the two controllers are observed with lifetime control scheme reducing the deflections with a standard deviation of 13.9%. In Figure 13(b), when the

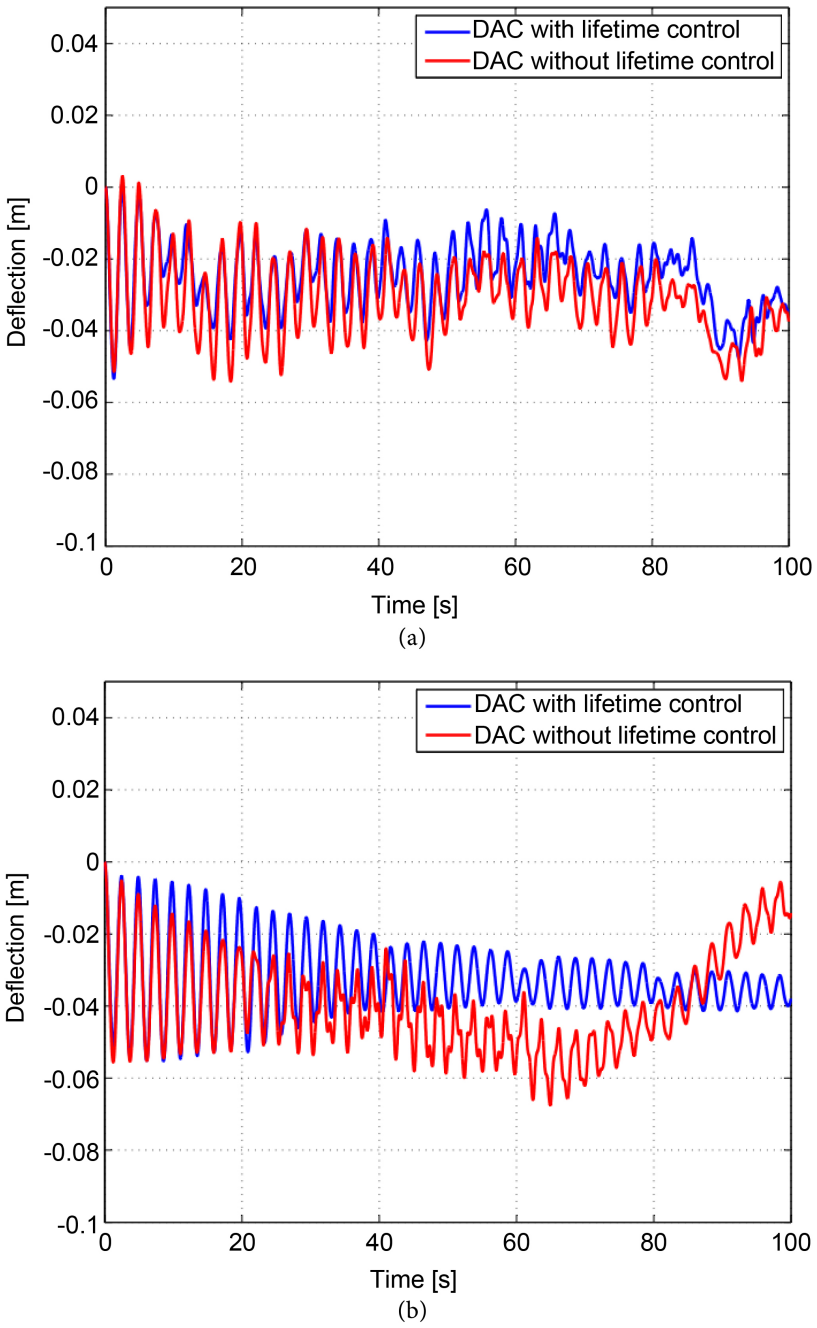

Figure 13. Tower side-to-side deflection. (a) Tower side-to-side deflection (stochastic wind). (b) Tower side-to-side deflection (step wind).

DAC without lifetime control is in use, significant fluctuations on tower side-to-side deflection are detected. The side-to-side deflections decrease for a while and begin to increase as the wind speed changes to higher wind speeds. However, when the lifetime control scheme is employed, deflections continuously reduce in size with fewer fluctuations even when wind speed increases. The improvement in the tower side-to-side deflection illustrated in **Figure 13(b)** is of a standard deviation of 28.3%.

Mitigation of blades' structural loads also impacts drivetrain loads due to the strong coupling between tower deflection and drivetrain vibration mode, to which the tower deflection mode is also strongly coupled to the blades' flapwise deflection mode. Investigation of the performance of the lifetime control on low speed shaft (LSS) tip moments is illustrated in **Figure 14**.

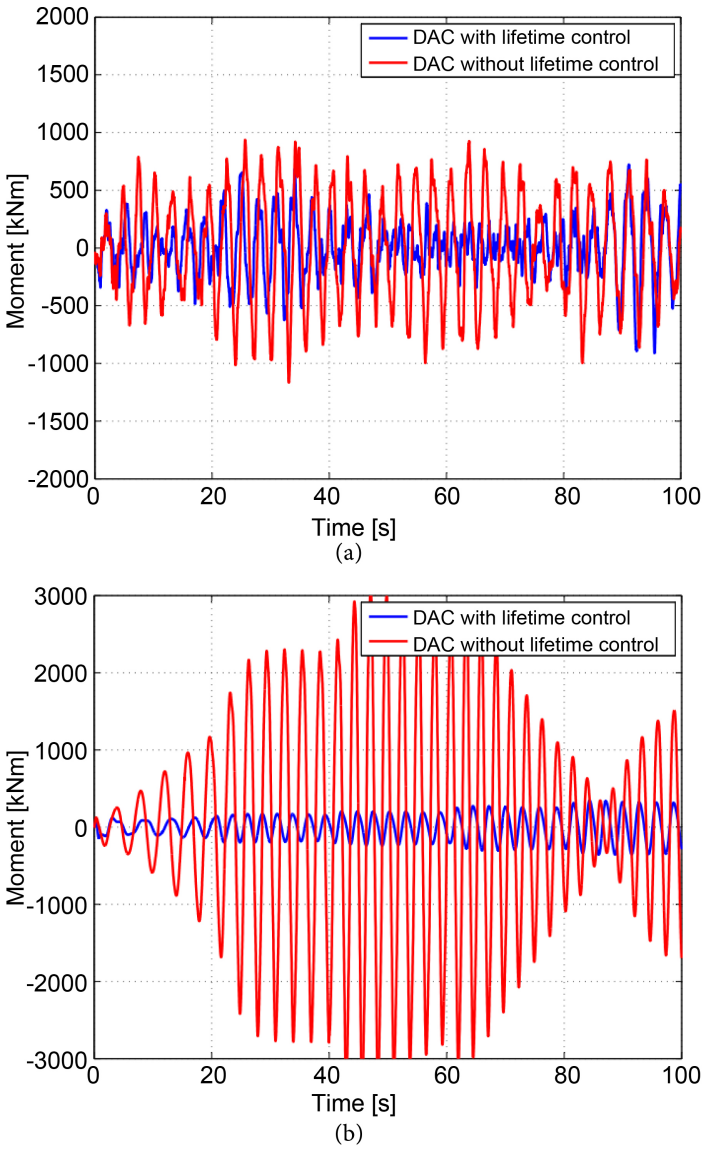

Figure 14. Drivetrain bending moments. (a) LSS shaft tip moments (stochastic wind). (b) LSS shaft tip moments (step wind).

A significant deviation between the two controllers in comparison is observed in **Figure 14(a)**, with the LSS tip moments reducing when the lifetime control strategy is employed. A reduction in LSS tip moments is realized with a standard deviation of 43.7% as shown in **Figure 14(a)**. In **Figure 14(b)**, when the DAC without lifetime control is employed, the moments have large fluctuations and tend to increase at every step; wind speed increases up to about 60 seconds, where the moments begin to significantly reduce, then increase again at about another step wind speed increase. Whereas, with lifetime control, the LSS tip moments regulation is stable with fewer fluctuations, although a slight increase in moments is detected at every step wind speed increase. The lifetime control significantly reduces the LSS tip moments with a standard deviation of 81.7%. Studies by [19] also present the impact of flapwise rotor blade bending moment on the drivetrain.

6. Conclusion

A real-time damage evaluation model integrated with a lifetime control (DAC) consisting of individual pitch controllers with different load reduction capabilities is presented in this paper. The results demonstrate PI-Observer efficiency in wind speed estimation as the estimated wind speed plot generally tracks the actual wind speed. The control scheme demonstrates significant effectiveness in the reduction of damage accumulation and blade bending moments as the bending moments reduce with a standard deviation of 15.9% with stochastic wind profile and 72.6% with step wind profile. The results of the study also show improvement in several wind turbine subsystems, such as in tower moments and in drivetrain (LSS) tip moments. Therefore, the study demonstrates that control of moments in rotor blades is significant in other wind turbine subsystems due to the strong coupling between various modes and components in a wind turbine. Efficient load mitigation and speed/power regulation are also realized by the control strategy as the results show output power regulation about the rated power value. This ultimately delays degradation and enables the wind turbine to be functional for the designed lifetime. Optimal maintenance scheduling becomes practical, especially for wind turbines that tend to be challenging to maintain if a random breakdown is to occur, such as in offshore wind turbines hence reducing maintenance costs. Though a linear damage accumulation model is adopted in this paper, fault propagation tends to be nonlinear in wind turbines and thus the nonlinear dynamics of damage accumulation can be considered in the future.

Acknowledgements

The authors acknowledge support from the Pan African University, Institute for Basic Sciences, Technology, and Innovation for funding the study.

Conflicts of Interest

The authors declare no conflicts of interest regarding the publication of this paper.

References

[1] Jain, T. and Yamé, J. (2020) Health-Aware Fault-Tolerant Receding Horizon Control of Wind Turbines. *Control Engineering Practice*, **95**, Article ID: 104236. https://doi.org/10.1016/j.conengprac.2019.104236

[2] Escobet, T., Puig, V. and Nejjari, F. (2012) Health Aware Control and Model-Based Prognosis. 2012 20*th IEEE Mediterranean Conference on Control & Automation* (*MED*), Barcelona, 3-6 July 2012, 691-696. https://doi.org/10.1109/MED.2012.6265718

[3] El-Thalji, I. and Jantunen, E. (2012) On the Development of Condition Based Maintenance Strategy for Offshore Wind Farm: Requirement Elicitation Process. *Energy Procedia*, **24**, 328-339. https://doi.org/10.1016/j.egypro.2012.06.116

[4] Musallam, M. and Johnson, C.M. (2012) An Efficient Implementation of the Rainflow Counting Algorithm for Life Consumption Estimation. *IEEE Transactions on Reliability*, **61**, 978-986. https://doi.org/10.1109/TR.2012.2221040

[5] Njiri, J. G., Liu, Y. and Söffker, D. (2015) Multivariable Control of Large Variable-Speed Wind Turbines for Generator Power Regulation and Load Reduction. *IFAC-PapersOnLine*, **48**, 544-549. https://doi.org/10.1016/j.ifacol.2015.05.035

[6] Zhang, Y., Chen, Z. and Cheng, M. (2013) Proportional Resonant Individual Pitch Control for Mitigation of Wind Turbines Loads. *IET Renewable Power Generation*, **7**, 191-200. https://doi.org/10.1049/iet-rpg.2012.0282

[7] Zhang, Y., Chen, Z., Cheng, M. and Zhang, J. (2011) Mitigation of Fatigue Loads Using Individual Pitch Control of Wind Turbines Based on FAST. 2011 46*th International Universities' Power Engineering Conference* (*UPEC*), Soest, 5-8 September 2011, 1-6.

[8] Bossanyi, E.A., Kumar, A. and Hugues-Salas, O. (2014) Wind Turbine Control Applications of Turbine-Mounted LIDAR. *Journal of Physics*: *Conference Series*, **555**, Article ID: 012011. https://doi.org/10.1088/1742-6596/555/1/012011

[9] Jelavić, M., Petrović, V. and Perić, N. (2010) Estimation Based Individual Pitch Control of Wind Turbine. *Automatika*: *Journal for Control*, *Measurement*, *Electronics*, *Computing and Communications*, **51**, 181-192. https://hrcak.srce.hr/56350 https://doi.org/10.1080/00051144.2010.11828370

[10] Jonkman, J.M. and Buhl, M.L. (2005) FAST User's Guide. National Renewable Energy Laboratory, Golden, Vol. 365, 366.

[11] Bir, G.S. (2010) User's Guide to MBC3: Multi-Blade Coordinate Transformation Code for 3-Bladed Wind Turbine. https://doi.org/10.2172/989416 https://digitalscholarship.unlv.edu/renew_pubs/57

[12] Wright, A.D. and Fingersh, L.J. (2008) Advanced Control Design for Wind Turbines; Part I: Control Design, Implementation, and Initial Tests (No. NREL/TP-500-42437). National Renewable Energy Lab. (NREL), Golden. https://doi.org/10.2172/927269

[13] Wright, A.D. (2003) Modern Control Design for Flexible Wind Turbines. University of Colorado, Boulder. https://doi.org/10.2172/15011696

[14] Ragan, P. and Manuel, L. (2007) Comparing Estimates of Wind Turbine Fatigue Loads Using Time-Domain and Spectral Methods. *Wind Engineering*, **31**, 83-99. https://doi.org/10.1260/030952407781494494

[15] Sawyer, S., Teske, S., Fried, L. and Shukla, S. (2014) Global Wind Energy Outlook.

[16] Ziegler, L., Gonzalez, E., Rubert, T., Smolka, U. and Melero, J.J. (2018) Lifetime Extension of Onshore Wind Turbines: A Review Covering Germany, Spain, Denmark,

and the UK. *Renewable and Sustainable Energy Reviews*, **82**, 1261-1271. https://doi.org/10.1016/j.rser.2017.09.100

[17] Kipchirchir, E., Do, M.H., Njiri, J.G. and Söffker, D. (2021) Prognostics-Based Adaptive Control Strategy for Lifetime Control of Wind Turbines. *Wind Energy Science Discussions*, 1-16. https://doi.org/10.5194/wes-2021-144

[18] Njiri, J.G., Beganovic, N., Do, M.H. and Söffker, D. (2019) Consideration of Lifetime and Fatigue Load in Wind Turbine Control. *Renewable Energy*, **131**, 818-828. https://doi.org/10.1016/j.renene.2018.07.109

[19] Beganovic, N., Njiri, J.G. and Söffker, D. (2018) Reduction of Structural Loads in Wind Turbines Based on an Adapted Control Strategy Concerning Online Fatigue Damage Evaluation Models. *Energies*, **11**, 3429. https://doi.org/10.3390/en11123429

[20] Liu, Y. and Söffker, D. (2009) Improvement of Optimal High-Gain Pi-Observer Design. 2009 *IEEE European Control Conference* (*ECC*), Budapest, 23-26 August 2009, 4564-4569. https://doi.org/10.23919/ECC.2009.7075120

[21] Njiri, J.G., Liu, Y. and Söffker, D. (2014) Disturbance Attenuation Using Proportional-Integral-Observer for Wind Turbine Speed Regulation. *Dynamic Systems and Control Conference*, Vol. 46209, V003T53A005. https://doi.org/10.1115/DSCC2014-6003

[22] Wang, N., Wright, A.D. and Balas, M.J. (2017) Disturbance Accommodating Control Design for Wind Turbines Using Solvability Conditions. *Journal of Dynamic Systems, Measurement, and Control*, **139**, Article ID: 041007. https://doi.org/10.1115/1.4035097

[23] Sinner, M. and Pao, L.Y. (2020) Revisiting Disturbance Accommodating Control for Wind Turbines. *Journal of Physics: Conference Series*, **1618**, Article ID: 022021. https://doi.org/10.1088/1742-6596/1618/2/022021

[24] Do, M.H. and Söffker, D. (2022) Wind Turbine Robust Disturbance Accommodating Control Using Non-Smooth H∞ Optimization. *Wind Energy*, **25**, 107-124. https://doi.org/10.1002/we.2663

[25] Dimitrov, N., Natarajan, A. and Kelly, M. (2015) Model of Wind Shear Conditional on Turbulence and Its Impact on Wind Turbine Loads. *Wind Energy*, **18**, 1917-1931. https://doi.org/10.1002/we.1797

[26] Beganovic, N., Njiri, J.G. and Söffker, D. (2017) Wind Turbine Control Strategy Deployment Concerning Remaining Useful Lifetime Prognostic Model. *Conference for Wind Power Drives*, Aachen, 7-8 March 2017, 1-8.